

# Aerodynamic Drag Force Analysis for Light Commercial Vehicle

M. H. Tonpe

Mechanical Department (Automotive Engineering)  
Sinhgad College of Engineering  
Pune, Maharashtra

A.P. Tadamalle

Mechanical Department  
Sinhgad College of Engineering  
Pune, Maharashtra

D. H. Burande

Mechanical Department  
NBN Sinhgad School of Engineering  
Pune, Maharashtra

**Abstract**— Aerodynamic drag is considered as the main obstacle to accelerate the solid body when it moves in the air. It deals with the study of stationary objects with the moving air, or in a motion on which the forces are acting by the air on the object. This paper describes the assessment of aerodynamic drag of LCV (Light commercial vehicle-Tata Winger) with the basic dimensions and modified changes in the exterior design of the vehicle. SolidWork tool is used for designing the CAD models while Ansys is used for the simulation to find the drag values. Three different models are made and simulation is carried out. The drag at different velocity ranging from 5 m/s to 25 m/s is calculated for the vehicle model. For better drag reducing compatible model all the three models are compared to each other with the drag values obtained through the simulation done in Ansys (Fluent). Experiment is performed in a subsonic wind tunnel with the model which shows better results in terms of drag. By using ansys it is easier to find the aerodynamic properties, time and material both are saved using this process.

**Keywords**—Aerodynamics, Computational fluid dynamics, Drag coefficient, Drag Force, Fuel efficiency, Tata winger, Vehicle design.

## I. INTRODUCTION

Aerodynamics is a field of fluid dynamics and gas dynamics which shares the theory between them. Aerodynamics can also be said the study of passing the air flow over the vehicle body and also studying the behavior of the flow with the use of CFD approach respectively. The aerodynamic properties of the vehicle body effects the performance, comfort and safety of the vehicle. While designing a vehicle the aerodynamic concept holds an important part. A drag reduced vehicle is only acceptable during the design of vehicle. Aerodynamic drag is considered as one of the main obstacle to accelerate the solid body when it moves in the air. Researchers have used the CFD techniques to perform numerical simulations related to the automobile.

The study in this paper presents the development process of aerodynamic in the vehicle external body. Various simulations are carried out to analyze the pressure field, velocity vector field, and aerodynamic force prediction related to a LCV. The stability of the aerodynamic forces caused by the airflow outside the car is identified. After that, the modification to the vehicle body that leads to lower wind drag was carefully evaluated. Experimentation is done in a subsonic wind tunnel using the model which gives better

results in terms of drag. The model used is scaled according to the dimensions of the wind tunnel available for the experimentation.

An aerodynamic car consumes less fuel and also overcomes the drag exerted by air when running at high speed and it provide good stability and handling behavior [1]-[2]. The reduction technique of aerodynamic drag can be used in all types of vehicles like cars, busses, vans, sports car etc. The aerodynamic drag on LCV is very less researched. Aerodynamic drag consist mainly two component skin friction drag and pressure drag. Among the total aerodynamic drag Pressure drag account most which depends on the external geometry due to boundary layer flow separation from rear window surface and wake region generated behind the vehicle body [3]. The two major part of aerodynamics are external aerodynamics and internal aerodynamics. External aerodynamics deals with the flow of air over the solid body having different shapes. While the internal aerodynamics deals with the flow that passes through inner compartment of solid body. The flow around a car is asymmetric due to which there is a separation region generated at the rear end of the vehicle. There are two different type of separation which occur (a) Quasi-two dimensional which occurs at the edge of the vehicle between grill and hood. It is characterized by high degree of turbulence. (b) Three dimensional separations which occur around the edges of the vehicle body where the air flows with an angle [4].

## II. CAD MODELLING

The model of vehicle used is a replica of Tata-winger which is used as ERV and also for passenger vehicle. The dimension of the vehicle is as 4520 mm in length, 1560 mm in width and 2050 mm in height. The model used for the project work is scaled to the ratio of 1:30 according to the wind tunnel dimensions. The wind tunnel dimension used for the analysis is of cross sectional area 100 cm x 30 cm x 30 cm. The CAD model with all the modification is shown in the Fig.1 (a, b, and c) as below.

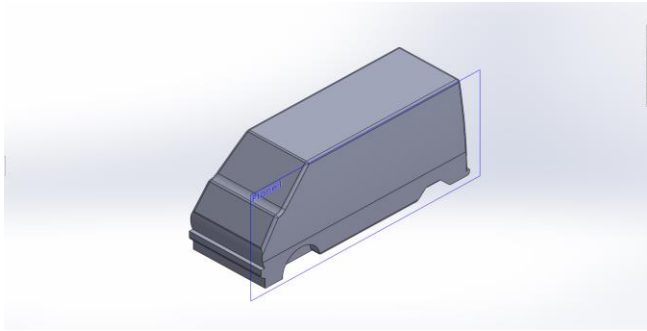


Fig. 1 (a) Base Model

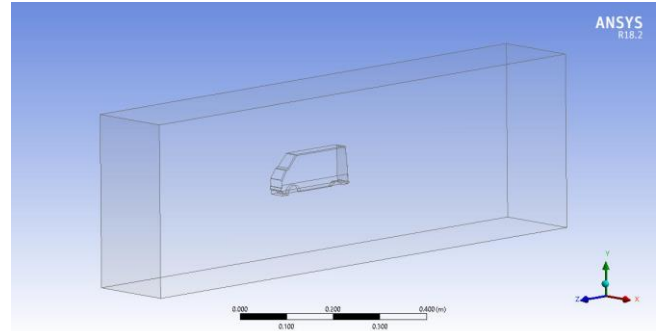


Fig. 2(a) Wind Tunnel Orientation

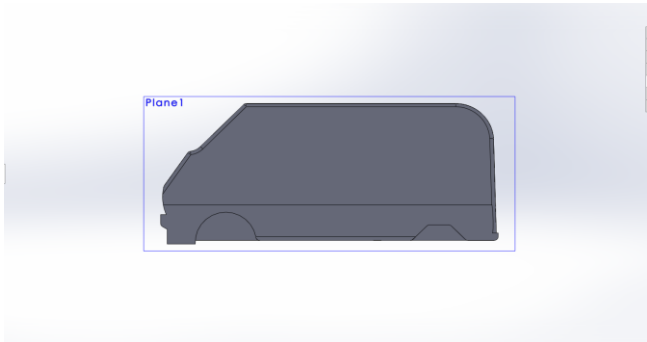


Fig. 1(b) Modified Model with Upper Rear End Cut

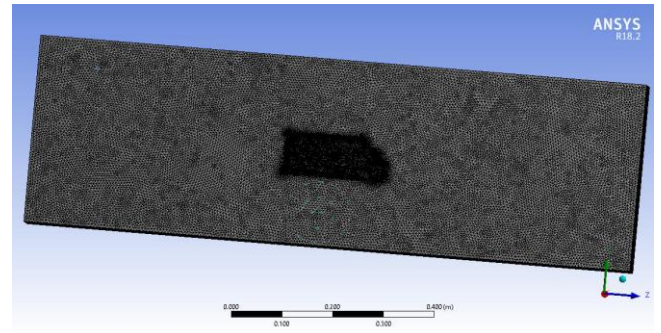


Fig. 2(b) Meshed Base Model

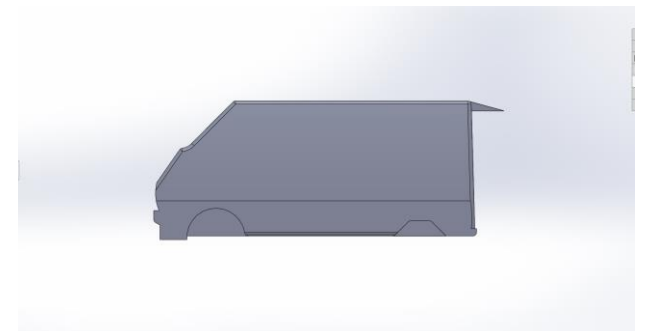


Fig. 1 (c) Modified Model with upper Rear End Tale Plate

The first modification is done with an upper rear cut of 508 mm in radius. Second modification is done by attaching an upper rear tale plate of 508 mm in length which has an inclination of 15° from the top surface.

### III. CFD ANALYSIS

The models made are mesh in the software and analysis is done using CFD (Fluent) approach to find the drag coefficient and drag force. The effect of wheels, side mirrors, and rear surface body parts are not studied in this paper. The side friction is so less that if not considered then also the value of drag obtained is acceptable for the particular shape of the body.

The remaining two models are also meshed in the same way as done for the base model. CFD analysis of the test model provides the result of drag coefficient and drag forces. [6] Boundary conditions are applied as the velocity inlet where the readings are calculated using different air velocities (5, 10, 15, 20, 25 m/s) and constant pressure outlet at atmospheric pressure 1 atm. [7]. A steady state incompressible Navier-stokes equation is obtained by implementing turbulent modeling with realizable k-epsilon (2 equations) and non-equilibrium wall function. Second order upwind discretization method is used in the solution method which goes to a peak value at first and then gives accurate result.

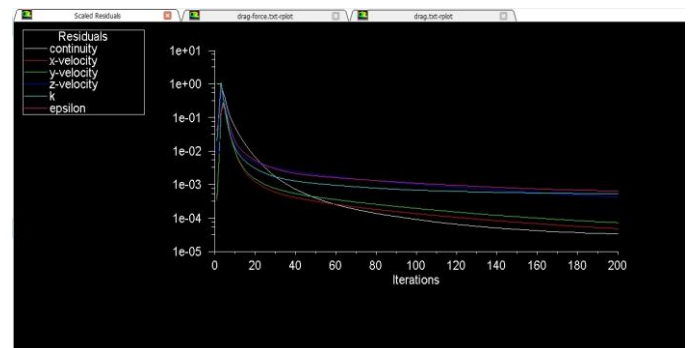


Fig. 3 Processing`

A. CFD Analysis of base model

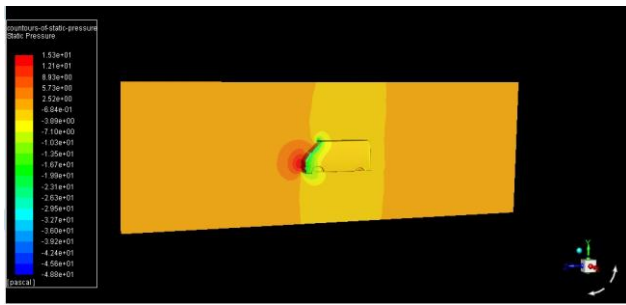


Fig. 4 Contours of Static Pressure

From Fig.4 it is seen that the maximum pressure occurs at the front of the vehicle. The maximum Static pressure acting on the model is 15.3pascal which is at the front surface of the model.

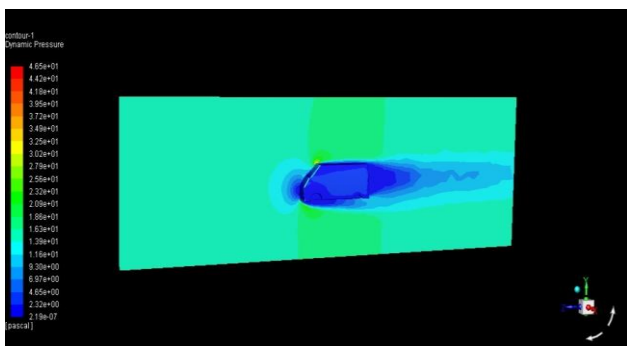


Fig. 5 Dynamic Pressure

Fig.5 represents the dynamic pressure of the base model. The maximum pressure acting on the model is 4.65pascal which acts at the front surface of the model.

B. Velocity Analysis of base model

Fig. 6(a and b) show the velocity streamline at different velocities 10 m/s and 20 m/s for the base model. Similarly velocity streamline for 5m/s, 15 m/s, and 25 m/s are also calculated.

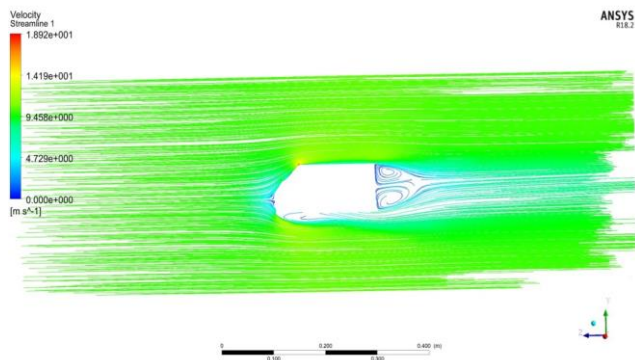


Fig. 6(a) Velocity Streamline at 10m/s

From the above Fig. 6(a) it is observed that the wake region is generated at the rear end of the vehicle. This wake region is the reason for the drag of vehicle. The air flow at this region is in separated form which decreases the pressure at the rear end.

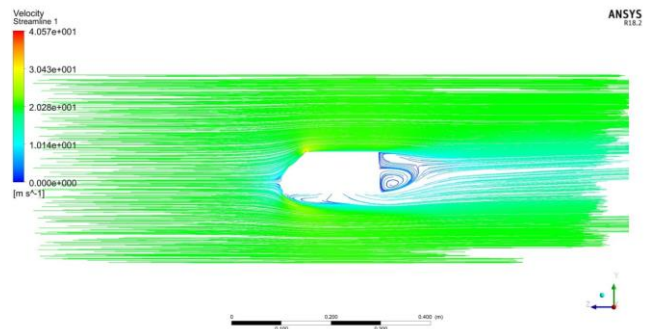


Fig. 6(b) Velocity Streamline at 20m/s

From the Fig. 6(b) it is seen that the wake region is reduced to some extent as the velocity increases but with increase in velocity the shape of the wake region also changes. The flow at the upper rear end of the vehicle at 20 m/s is different as compared to the velocity at 10 m/s. The results obtained from the analysis are shown in Table I as shown below.

Table I: Result of base model using Ansys

Velocity (m/s)	Velocity (km/hr.)	Drag Coefficient	Drag Force (N)
5	18	0.60863	0.026219
10	36	0.54712	0.094278
15	54	0.51118	0.19819
20	72	0.49916	0.34406
25	90	0.48887	0.5265

C. Velocity Analysis of Modified Model with upper rear end cut.

Fig. 7(a and b) show the velocity streamline for the modified model with upper rear end cut of 508 mm radius.

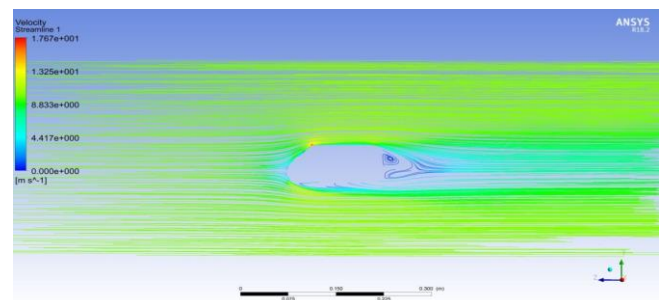


Fig. 7(a) Velocity Streamline at 10m/s

From Fig. 7(a) it is seen that the wake region generated for the model is different from the base model at similar velocity. The velocity streamline after the wake region also shows the decrease in velocity in that region.

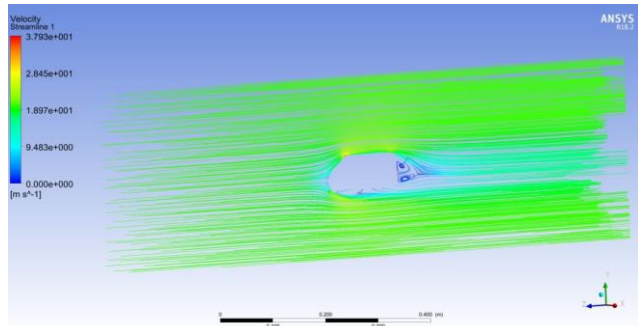


Fig. 7(b) Velocity Streamline at 20m/s

When the velocity is increased for this model the wake region generated is small but with more space area behind the vehicle which has less pressure as compared to the front. This increases the drag force of the vehicle. The analysis results of drag force and coefficient are shown in the Table II for the first modification done to the base model.

Table II: Result of modified model with upper rear end cut using Ansys

Velocity (m/s)	Velocity (km/hr.)	Drag Coefficient	Drag Force (N)
5	18	0.6616	0.01619
10	36	0.53721	0.052582
15	54	0.5075	0.111767
20	72	0.5043	0.19745
25	90	0.49806	0.30468

**D. Velocity Analysis of Modified Model with upper rear end cut.**

Fig. 8 (a and b) show the velocity streamline of the modified model with upper rear end tale plate with 508 mm in length and 15° inclination from the top surface.

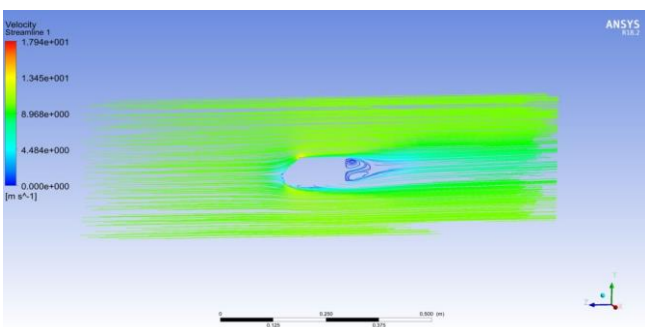


Fig. 8(a) Velocity Streamline at 10m/s

It is seen from the above Figure 8(a) that the wake region generated by the modified model at the rear end of the vehicle is close to the upper rear end of the vehicle due to which the flow of the air is attached to the surface of the vehicle.

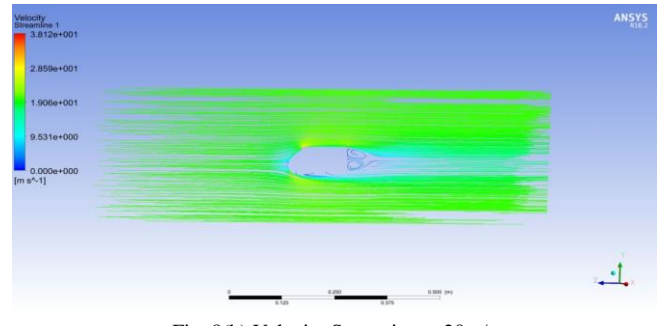


Fig. 8(b) Velocity Streamline at 20m/s

All the figures shows the flow of velocity over the surface of the base model and modified models. Its seen that at each velocity there is a different formation of wake region at the rear end of the vehicle. The results obtained for the second modification done to the base model are shown in the Table III. Velocity vector colored by velocity magnitude can also be obtained from this analysis for all the different velocities for all the three models of vehicle. Its is seen that the separation of flow takes a the rear end of the vehicle due to which the wake region is generated. The formation of wake region is different at different velocities.

Table III: Result of modified model with upper rear end tale plate using Ansys

Velocity (m/s)	Velocity (km/hr.)	Drag Coefficient	Drag Force (N)
5	18	0.60562	0.01489
10	36	0.53015	0.05189
15	54	0.49723	0.1095
20	72	0.48567	0.19014
25	90	0.47861	0.292785

From the results obtained through the analysis the second modification of rear tale plate attachment shows better drag reducing capability as compared to the base model and first modification done to the vehicle. Hence the vehicle model with second modification done to the base model is used for the experimentation.

**IV. EXPERIMENTAL METHOD**

The experimental test was carried out using a subsonic wind tunnel of cross section 100 cm x 30 cm x 30 cm. The model was placed at a height of 14.2cm from the bottom of the wind tunnel. An anemometer was placed at the rear end of the model to measure air flow velocity. Readings were taken at different velocity for the modified model with rear tale plate attachment as it gives us the good results compare to the other model as per the simulation work done. The following Figure shows us the Experimental setup of the wind tunnel.

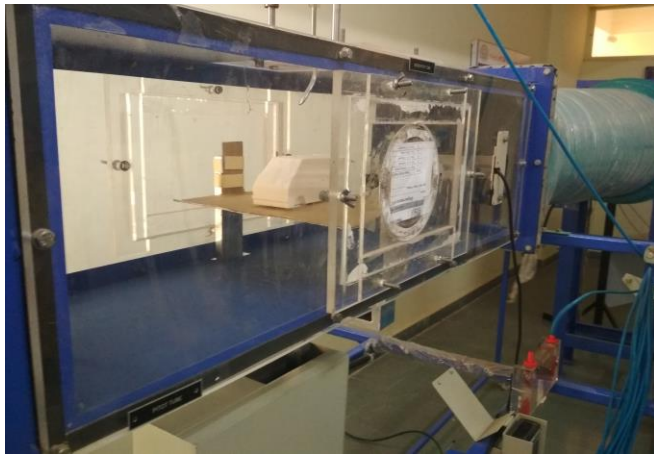


Fig. 9 Wind tunnel Experimental Setup

The setup was connected to a pitot tube and anemometer which is used to calculate the Drag force as shown in the Figure 10.



Fig. 10 Wind Tunnel Setup with Annemometer

The experimental formula to calculate the drag coefficient is given by,

$$\text{Drag } (C_d) = \frac{2 \cdot F_D}{\rho V^2 A}$$

Where,  $C_d$  is Coefficient of drag,  $F_D$  is Drag force,  $\rho$  is Density of air,  $V$  is Velocity of air, and  $A$  is the frontal area of the vehicle [1]. The drag values for different velocities are calculated for the second modified model and compared with the simulation results obtained. The results obtained by the experiment performed for the modified model are shown in below Table IV.

Table IV: Experimental Results of the Modified Model.

Velocity (m/s)	Velocity (km/hr.)	Drag Coefficient	Drag Force (N)
5	18	0.6130	0.03
10	36	0.5108	0.05
15	54	0.59031	0.13
20	72	0.4342	0.17
25	90	0.408676	0.25

## V. RESULTS AND DISCUSSION

From the analysis of the models it is observed that when the flow is separated it gets reattach further downstream. This type of separation occurs at the rear side of the vehicle and a big wake region is generated behind the car. The circulation depends upon the shape of the edge where separation occur and the direction of the air that moves from the high pressure region to low pressure region. When a fluid flows around the body it slows down nearest to the body due to the friction with the surface. The decreased velocity of air results in an increased pressure on the surface which means that the force to slow down the vehicle increases to the force to carry the vehicle forward. A wake is created at the place of separation which has low pressure then the surrounding. The low pressure behind the vehicle is a combination with the high pressure in front of it which leads to the increase in drag resistance.

The drag coefficient and drag force at different velocities for all the models of the vehicle are calculated. The drag values obtained in the Table I, II, and III shows that the drag coefficient is affected by change in velocity. From the results obtained it is also observed that as the velocity increases the drag force also increases.

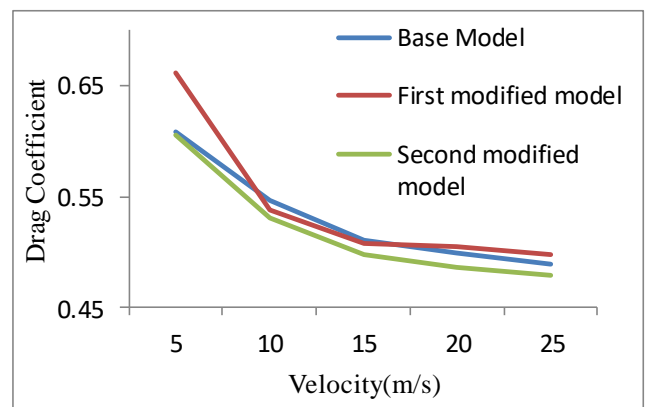


Fig. 11 Drag Coefficient with Change in Velocity

The graph of drag coefficient and velocities is plotted for all the three models. It is seen that the modified model with the upper rear tale plate attachment reduces the drag at some extent which can be considered as good from the aerodynamic point of view. The experimental results are calculated for the modified model with rear tale plate attachment and compared with the simulation results for validation. It is seen that the values matches well with the simulation results for the series of velocity. The minor changes in the values are due to the mesh generation and grid size used in the computational method [2].

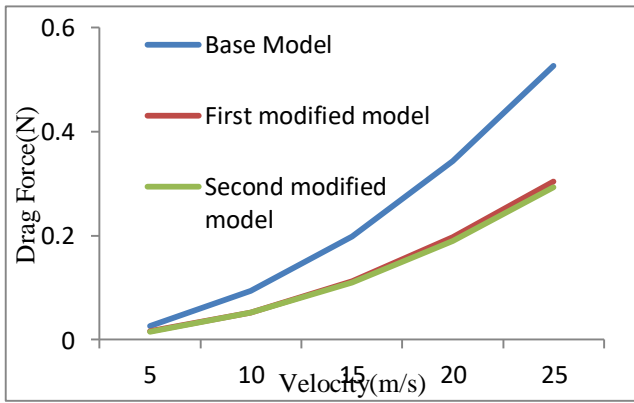


Fig. 12 Drag Force with Change in Velocity

The graph of drag force and drag coefficient with change in velocity obtained by experimental method and computational method for the second modified model with rear tale plate attachment is shown in Fig. 13 and Fig. 14 respectively.

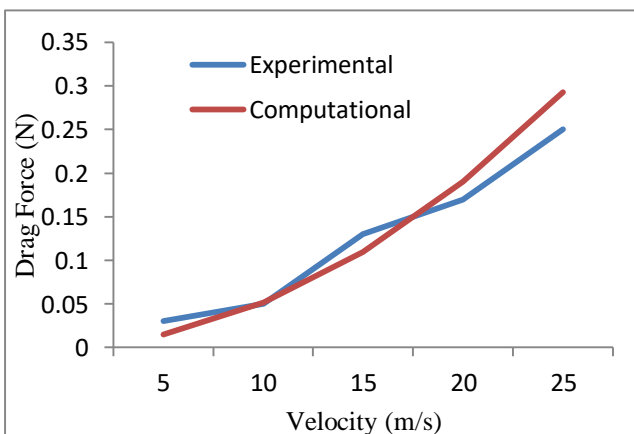


Fig. 13 Experimental and Computational Drag Force

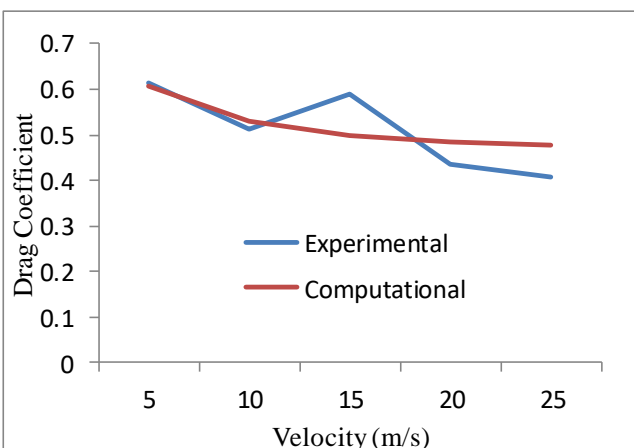


Fig. 14 Experimental and Computational Drag Coefficient

## VI. CONCLUSION

From the results it can be concluded that the drag is affected by change in velocity. Drag force increase with increase in velocity. Among the two modifications the second modification with rear tale attachment shows better drag reducing capability as compared to the base model and first modified model. The computational value matches well with the experimental values performed for the modified model. The percentage reduction of 2.17% is obtained from the results by implementing the second modification for the base model. It is also seen that these types of changes can be used to improve the drag of the different light commercial vehicles. A small reduction in aerodynamic drag of a vehicle gives better performance and handling behavior of the vehicle.

## REFERENCES

- [1] Dinesh Dhande, Manoj Bauskar, "Analysis of Aerodynamic Aspects of SUV by Analytical and Experimental Method", International Journal of Emerging Technology and Advanced Engineering, Vol. 03, Issue 07, 2013, pp. 447-451.
- [2] Manan Desai, S.A. Channiwala, H.J.Nagarsheth, Experimental and Computational Aerodynamic Investigation of a Car, International Conference on Fluid Mechanics and Aerodynamics, Rhodes, Greece, Vol. 03, Issue 04, 2008, pp. 359-368.
- [3] Darshan M.Desai, Imran Molvi, Effect of various aerodynamic drag reduction methods on vehicle- A Review, International journal of advance engineering and research development, Vol. 04, Issue 06, 2017, pp. 214-220.
- [4] Rikard Rigdal, Johan Levin, "Aerodynamic analysis of drag reduction devices on the under body for SAAB 9-3 by using CFD", Department of applied mechanics, Division of vehicle engineering and autonomous systems Chalmers University of technology. (2011) 2-10,
- [5] S.M. Rakibul Hassan, Toukir Islam, Mohammad Ali, Md. Quamrul Islam, "Numerical Study on Aerodynamic Drag Reduction of Racing Cars", International Conference on Mechanical Engineering, Elsevier Procedia Engineering, 2014, pp. 308-313.
- [6] Senan Thabet, Thabit H. Thabit, "CFD Simulation of the Air Flow around a Car Model (Ahmed Body)", International Journal of Scientific and Research Publications, Vol. 08, Issue 07, 2018, pp. 2182-2186.
- [7] V. Naveen Kumar, K. L. Narayan, L. N. V. Narasimha Rao and Y. Sri Ram, "Investigation of Drag and Lift Forces over the Profile of Car with Rear spoiler using CFD", International Journal of Advances in Scientific Research, Vol. 01, Issue 08, 2015, pp-331-339.
- [8] <https://youtu.be/dZR7Wi70Vec>